Interactive Eye Aberration Correction for Holographic Near-Eye Display

Kenta Yamamoto
University of Tsukuba
Tsukuba, Japan

Ippei Suzuki
University of Tsukuba
Tsukuba, Japan

Kosaku Namikawa
University of Tsukuba
Tsukuba, Japan

Kaisei Sato
University of Tsukuba
Tsukuba, Japan

Yoichi Ochiai
University of Tsukuba
Tsukuba, Japan

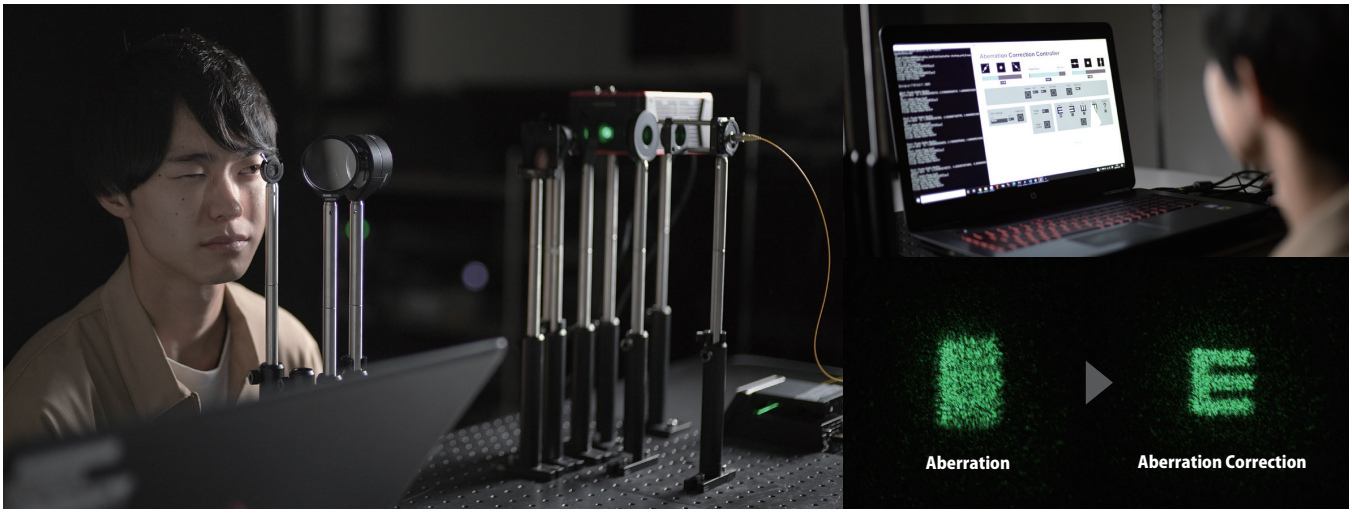

Figure 1: (left) Setup of proposed aberration-correctable holographic near-eye display and its user. (right above) The interface for aberration correction adjustment. (right below) The result of aberration correction that compensates distorted images.

ABSTRACT

Distortions of observed images have been a long-standing problem in near-eye displays. Although many correction methods for optical system-dependent aberrations have been proposed, the image distortions caused by eye aberrations have not been studied thoroughly. In addition to the problem, eye aberrations are individual specific. Therefore, a system capable of correcting the aberration irrespective of the individual is necessary. In this study, we propose an aberration-correctable holographic near-eye display (HNED) that can be used to interactively compensate for image distortions caused by eye aberrations. We formulate a propagation equation that includes eye aberrations in the HNED and developed a GUI that enables a user to correct eye aberrations on their own. In this system, the image displayed on the HNED is updated based on the correction coefficients specified by the user. We performed experiments on human subjects to verify the effectiveness of the proposed method. Our results indicate that the minimum identifiable size in our HNED can be reduced by the aberration correction using our interface, and especially our aberration correction method is useful for the visibility of low visual-acuity users.

AHs '21, February 22–24, 2021, Rovaniemi, Finland

CCS CONCEPTS

• **Computing methodologies** → **Mixed / augmented reality**; • **Human-centered computing** → *Displays and imagers.*

KEYWORDS

Near Eye Display, Eye Aberration, Aberration Correction, Computer-Generated Hologram

ACM Reference Format:
Kenta Yamamoto, Ippei Suzuki, Kosaku Namikawa, Kaisei Sato, and Yoichi Ochiai. 2021. Interactive Eye Aberration Correction for Holographic Near-Eye Display. In *Augmented Humans International Conference 2021 (AHs '21), February 22–24, 2021, Rovaniemi, Finland.* ACM, New York, NY, USA, 11 pages. https://doi.org/10.1145/3458709.3458955

1 INTRODUCTION

Near-eye display is an essential technology for realizing the virtual and/or augmented reality. It can provide various new visual

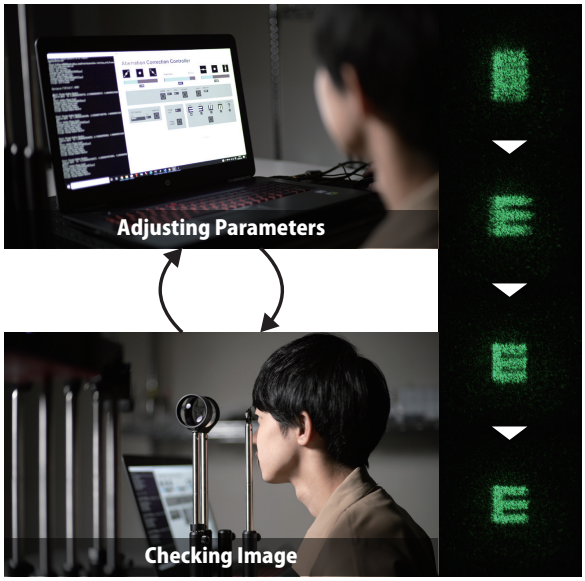

Figure 2: Process to correct the image distortions caused by eye aberrations. User can realize the aberration compensation by repeatedly checking the image and adjusting the correction parameters.

experiences. In particular, holographic near-eye display (HNED), which is based on holographic computation, is considered to be an important technology to display high resolution and 3D images. Various methods have been proposed in the past few years for the advancement of holographic display technologies.

Owing to the characteristics of the optical design, the near-eye displays have different design considerations than those of conventional displays. For example, it is necessary to consider the characteristics of the human eye, which is considered as a type of imaging optical system in which a group of lenses consisting of a cornea and crystalline lens forms the image on the retina. Aberrations are inherent in the eyes: myopia, hyperopia, and astigmatism are some common ones. If near-eye displays are not designed for aberration correction, it will be problematic for users who have eye problems that require eyeglasses.

The problem of eye aberrations has not been explored fully in the context of HNEDs. Maimone et al. [32] treated aberrations caused by the eye and the near-eye display as one "black box" and examined the importance and feasibility of aberration correction in HNED. Takaki et al. [43] studied the importance of aberration correction in a Maxwellian-type near-eye display and demonstrated the realization of the correction. These studies demonstrate only the results of aberration correction and do not provide a sufficient formulation of the eye aberration problem and aberration correction method. Kim et al. [22, 23] proposed a method for calculating the phase distribution on the spatial light modulator (SLM) with aberration correction by the ray tracing of the optical system including the eyes. However, previous studies have not demonstrated how a user could apply appropriate aberration correction.

Therefore, the research on aberration correction in near-eye displays is limited in terms of usability and feasibility. In this study, we propose an aberration-correctable HNED and a GUI to enable users to correct aberrations interactively. We used imaging simulations and actual optical systems to evaluate the proposed aberration-correctable HNED. The proposed aberration correction system has several coefficients for aberration correction, and the user can adjust each coefficient via an interface while checking the displayed image directly (Fig. 2). To test the effectiveness of the interface, we performed an experiment involving human subjects. The subjects were required to perform a task similar to the visual acuity test, which was aimed to demonstrate the quantitative improvement in the vision after the correction. The experimental results demonstrated that aberration correction was effective and considering the aberrations of the human eye could improve the quality of the image in HNED.

The main contributions of this study are the following:

- We formulated the propagation of light in the HNED, including aberrated eyes, and proposed a method for computing the wavefront that can compensate for the aberrations. We also built a benchtop prototype of the HNED.
- We have developed an interface that helps the users to correct aberrations interactively by themselves.
- We performed an experiment involving human subjects to verify the effectiveness of aberration correction using the aberration-correctable benchtop prototype of the HNED and GUI.

2 RELATED WORK

2.1 Measurement, Correction, and Simulation of Eye Aberration

Correct visual information is important for humans to live. Therefore, devices have been developed for those with poor or problematic eyesight. Technologies for the measurement and analysis of eye aberrations have been developed to quantify vision problems. For example, early studies on the measurement of vision were published more than two centuries ago, and the existence of spherical aberration in the human eye was recognized as early as 1801 [50]. Subsequent studies have advanced our understanding of the human eye aberrations. These include the studies to measure the eye aberrations as geometric aberration [45] and analyzing the aberrations using a subjective assessment [13, 14]. In contrast with these early methods, the wavefront aberration measurement using a Shack-Hartmann sensor led to a sudden improvement in the accuracy of the aberration measurement [12, 27, 28, 40]. This is an established method and has been incorporated into commercial aberration measurement products.

Along with establishing measurement methods, many aberration correction methods have also been developed. Eyeglasses are one of the most common methods of aberration correction. Because it is difficult to correct higher-order aberrations, a technology, such as contact lenses, capable of correcting such aberrations are required [36, 44, 46]. In addition to these two correction methods, various other methods of aberration correction have been proposed: using phase plates for aberration correction [35], incorporating

Table 1: Comparison with previous vision-correcting displays.

	Display Position	Display Type	GUI for User-defined Parameters	Real-time Aberration Measurement
Huang et al. (2011) [16]	Far-Eye Display	LCD	N/A	N/A
Fernandez et al. (2012) [9]	-	Adaptive Optics Visual Simulator	N/A	Available
Pamplona et al. (2012) [38]	Far-Eye Display	Light Field Display	N/A	N/A
Huang et al. (2012, 2014) [17, 18]	Far-Eye Display	Light Field Display	N/A	N/A
Maimone et al. (2017) [32]	Near-Eye Display	Holographic Display	N/A	N/A
Takaki et al. (2018) [43]	Near-Eye Display	Holographic Display	N/A	N/A
Kim et al. (2019, 2020) [22, 23]	Near-Eye Display	Holographic Display	N/A	N/A
Ours	Near-Eye Display	Holographic Display	Available	N/A

adaptive optics to correct aberrations in real-time while measuring eye aberrations [10], overlaying the compensation image with an optical see-through HMD [19], inserting intraocular lenses [1, 2], and corneal surgery using lasers [33].

Based on an improved understanding of the relationship between the aberration and visual field images, studies have been performed to simulate or experience how eye aberrations change the visual field image. Several methods, such as the point spread function (PSF) method [6, 47] and the rendering method [3, 7, 21, 37] have been used to simulate the visual field image with aberrations. As for the experienceable system for the aberrated visual field image, studies have used an optical system with built-in adaptive optics, called adaptive optics visual simulator (AOVS) that enables arbitrary aberrations to be delivered to the eye [4, 9, 41].

2.2 Vision-Correcting Display

People use displays naturally in their routines. This makes the comfort of viewing displays important for them. In the field of computational displays, a correction technique without eyeglasses for the visually impaired people has been developed. This technique is called "vision-correcting displays." An early method for computing the displayed image was proposed by Huang et al. [16]. Their method improves the visibility of the image by applying PSF to the displayed image, which is opposite to the aberration of the eyes. They also proposed a display method that achieves aberration correction by stacking multiple displays [17]. Later on, methods based on using light field displays for aberration correction have been proposed [18, 38].

2.3 Aberration Correction for Near-Eye Display

Image distortion due to aberration has been a problem in many near-eye displays. This problem is caused by optical system-dependent aberrations. Therefore, aberration correction methods have been considered [26, 29, 34, 49] to address this problem. Recent studies suggest that aberrations specific to optical systems can be compensated for by incorporating a camera into a feedback loop [5, 39].

Another important source of aberrations in near-eye displays is the human eye. Therefore, several studies have investigated eye aberrations in near-eye displays. Maimone et al. [32] considered both optical and eye aberrations together as a single aberration and described the feasibility and importance of aberration correction accordingly. Takaki et al. [43] described the effect of aberration in the Maxwellian-type near-eye display and presented the results of aberration correction. Although the aforementioned studies succeeded in demonstrating the results of aberration correction, they did not fully formulate the problem of eye aberration. Kim et al. [22, 23] defined the eye using a schematic eye model and established a method for calculating the phase distribution by adding aberration information to the ray tracing of the optical system including the eye. However, this method requires the precise shape of the eye of each user and cannot handle aberrations generally. Furthermore, there is no discussion on how users can actually adjust the aberration correction.

2.4 Position of Our Method

In Table 1, we summarize the existing methods that offer displays that adapt to eye aberrations. These studies can be divided into two types: far-eye and near-eye display studies. Most existing methods of both types do not offer a deeper insight into how the user actually adjusts for the aberration correction, and no GUI for handling correction parameters has been proposed. Although there are methods with real-time aberration measurements, such as AOVS, it is difficult to incorporate them into a near-eye display because the miniaturization of these measurement systems is difficult. Therefore, we propose a method for users to make their own corrections by providing a GUI.

3 PRINCIPLE

3.1 Light Propagation

HNED is a device that outputs images based on hologram calculations. Hologram computation is based on wave optics, which treats light as a wave; the computed hologram is called a computer-generated hologram. In wave optics, the state of the light is expressed in complex amplitudes. When dealing with the light propagation from one plane to another, we calculate the distribution of complex amplitudes on each plane. The source plane of the light propagation and the destination plane are defined as u_1 and u_2, respectively (Fig. 3(a)). In this study, we use the Fresnel diffraction propagation equation to calculate the light propagation. The Fresnel diffraction propagation from u_1 to u_2 is represented as following:

$$u_2(x_2, y_2) = \mathcal{F}^{-1}\left[\mathcal{F}\left[u_1(x_1, y_1)\right]\mathcal{F}\left[\exp\left(\frac{i\pi p^2}{\lambda z}\left(x_1^2 + y_1^2\right)\right)\right]\right] \quad (1)$$

where $\mathcal{F}$ is the Fourier transform, $\mathcal{F}^{-1}$ is the inverse Fourier transform, z is the distance between u_1 and u_2, λ is the wavelength, and p is the pitch size of the SLM.

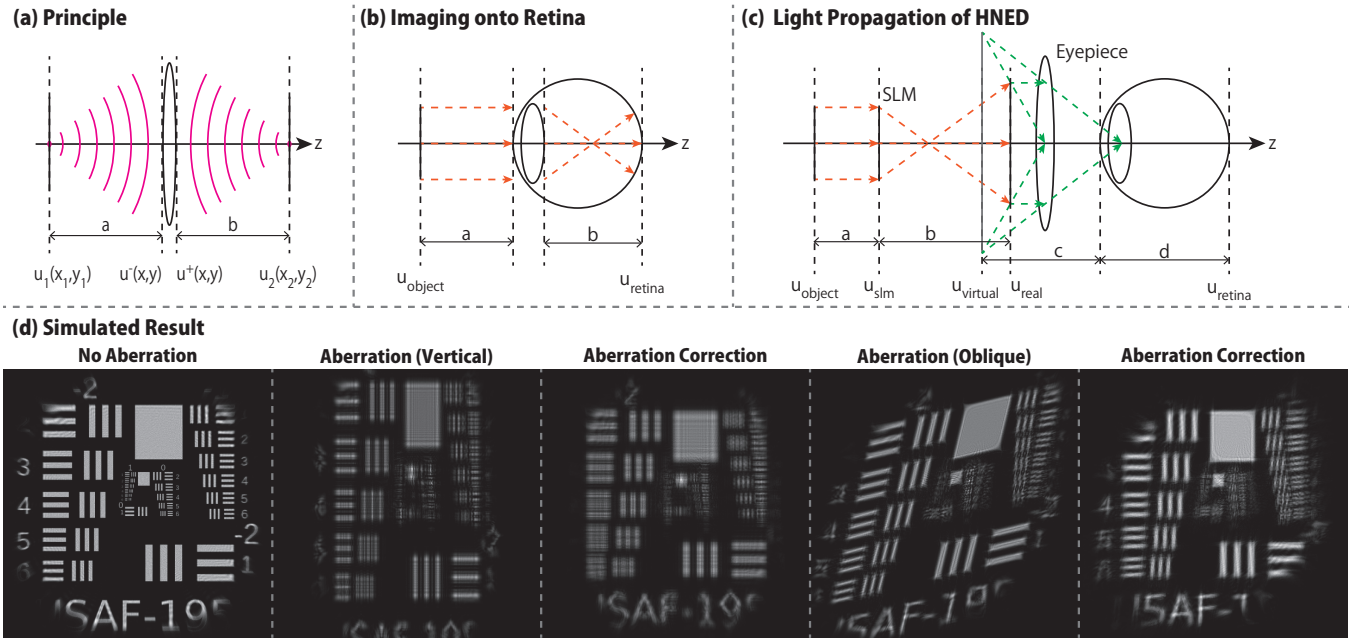

Figure 3: (a) Schematic of refocusing of a point light source with a lens. (b) Schematic of imaging on the retina by the eye lens. (c) Schematic of light propagation in our HNED, including SLM and eyepiece. The user observes the real image formed by the SLM as an imaginary optical system through the eyepiece. (d) Results of aberration correction simulated based on the light propagation formulated in (c).

3.2 Lens Imaging with Aberrations

The human eye is an optical imaging device. It consists of two lenses (the cornea and crystalline lens) and a sensor (the retina). In general, the role of the lens is to refocus a point light source (Fig. 3(a)). The following equation represents the distance relationship between the point light source and the refocus point:

$$\frac{1}{a} + \frac{1}{b} = \frac{1}{f} \tag{2}$$

where a is the distance between the point light source and the lens, b is the distance between the lens and the refocus point, and f is the focal length of the lens. Utilizing Eq. 1 for the light propagation from the point light source to the focal point, the converging feature of the lens can be defined as the following phase distribution $t(x, y)$:

$$t(x, y) = \exp\left(-i\frac{\pi}{\lambda}\left(\frac{x^2 + y^2}{f}\right)\right). \tag{3}$$

In such imaging optical systems, perceptible distortions occur owing to distortions by the lens. Similar to the optical lens, the human eye is also prone to distortion, which is commonly called astigmatism. Such a distortion is defined as a wavefront aberration in wave optics. Wavefront aberration is a measure of the distance between the ideal and distorted wavefronts. Wavefront aberration is generally expressed using the Zernike polynomial as follows:

$$W(x, y) = \sum_{j=0}^{N} \alpha_j Z_j \tag{4}$$

where $W(x, y)$ is the wavefront aberration, Z_j is the Zernike polynomial, and α is the Zernike coefficient.

Because these aberrations are caused by the lens, we must consider the aberrations in the lens equation. We include the aberration in the pupil function P and define it as the generalized pupil function $\mathcal{P}$:

$$\mathcal{P}(x, y) = P(x, y)\exp(ikW(x, y)) \tag{5}$$

where k is the wave number. Utilizing Eq. 3 and Eq. 5, the transformation equation for the complex amplitude distribution with an aberrant lens is defined as

$$u^+ = u^- * t(x, y) * \mathcal{P}(x, y) \tag{6}$$

where u^- and u^+ are the complex amplitude distributions at the front and behind the lens, respectively.

3.3 Calculating Phase Hologram on SLM

Recently, several optimization methods have been proposed to compute phase holograms on SLMs. In particular, it was demonstrated by Peng et al. [39] that automatic differentiation-based optimization is the best method for phase computation. However, it requires iterative processing, which is not suitable for fast processing, and cannot be incorporated into interactive systems. Therefore, we adopted the double-phase amplitude coding (DPAC) method, which computes the phase hologram directly. The principle of the DPAC method was proposed several decades ago [15]. Recently, a method for recovering complex amplitudes using a diffraction grating has been proposed [11, 30]. The working principle behind this method

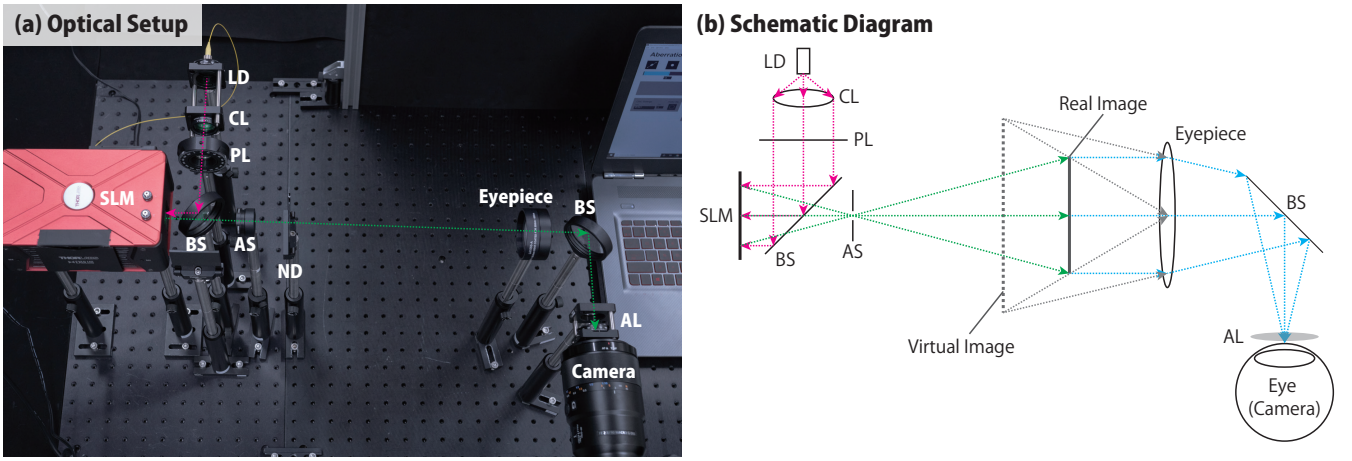

Figure 4: (a) Optical setup of the benchtop prototype of HNED. (b) Schematic of the optical setup. LD: laser diode; CL: collimator lens; PL: polarizer; BS: beam splitter; AS: aperture stop; ND: ND filter; AL: aberrated lens.

is that complex amplitudes can be recovered from two phases:

$$A\exp(i\theta) = \exp(i\theta_1) + \exp(i\theta_2) \tag{7}$$

where $\theta_1 = \theta + \arccos(\frac{A}{2})$ and $\theta_2 = \theta - \arccos(\frac{A}{2})$. This method enables to handle complex amplitudes even when using only phase SLMs. Maimone et al. [32] proposed a method for displaying two phases in a checkerboard pattern, each being equivalent to a single SLM. This method is also adopted in this paper.

4 EYE ABERRATION CORRECTION

4.1 Imaging Formula

We formulate the imaging optics of the eye in a near-eye display. In the human eye without any refractive error, the focal length of the lens coincides with the distance to the retina when the eye is focused at infinity. When observing an object closer than the infinity, the focal length of the eye lens changes such that Eq. 2 holds. For example, when the distance from the eye to the object is a and the distance from the lens of the eye to the retina is b (depicted in Fig. 3 (b)), the image of the object on the retina is given by the following propagation equation:

$$u_{retina} = Prop_b\ (Prop_a(u_{object}) * t(x,y) * \mathcal{P}(x,y)) \tag{8}$$

where $Prop_n()$ is the propagation computation in Eq. 1 at distance $z = n$.

4.2 Eye Aberration Correction Formula

An aberration-correctable HNED system using an eyepiece is depicted in Fig. 3(c). In this optical system, the real image u_{real} is observed using an eyepiece. Because this optical system uses a virtual image, we cannot simulate the imaging process appropriately with the wavefront propagation. Therefore, we ignore the image magnification of the virtual image in simulations and calculate the image formed on the retina by treating the virtual image as the real image.

The real image observed through the eyepiece is calculated such that the distortion of the image is opposite to the distortion caused by the eye lens. The phase distribution to be displayed on the SLM is derived from the following propagation calculation:

$$u_{slm} = Prop_a(u_{object}) * t(x,y) * \mathcal{P}_{rev}(x,y). \tag{9}$$

where $\mathcal{P}_{rev}(x,y)$ contains aberrations that are the opposite of eye aberrations. The real image to be observed through the eyepiece can be obtained from the following propagation formula:

$$u_{real} = Prop_b(u_{slm}). \tag{10}$$

In the simulation, the real image is formed on the retina along with the following propagation formula:

$$u_{retina} = Prop_d(Prop_c(u_{real}) * t(x,y) * \mathcal{P}(x,y)). \tag{11}$$

The results of the simulation are presented in Fig. 3 (d). In this simulation, we attempted to correct for vertical and oblique astigmatisms. As shown by these results, the aberration distortions can be corrected.

5 RESULT

In this section, we construct an optical system based on the propagation formula proposed in Section 4 and present the results of the aberration correction.

5.1 Optical Setup

The setup of the optical system is depicted in Fig. 4. The light source was a 520 nm laser beam (Thorlabs LP520-SF15[1]), which was collimated and then irradiated to the SLM through a linear polarizer, and an ND filter with an optical density of 2.0 was used to reduce the amount of light incident on the eye. The SLM used in this experiment was Thorlabs Exulus-4K-1/M[2], with a pitch of 3.74 μm and a pixel count of 3840×2160. In this study, the central 2160×2160 pixels were used to display the phase distribution. The SLM depicts the phase distribution calculated using Eq. 9. Because the phase pattern

[1]https://www.thorlabs.co.jp/thorproduct.cfm?partnumber=LP520-SF15 (last accessed Jan. 31, 2021)
[2]https://www.thorlabs.com/thorproduct.cfm?partnumber=EXULUS-4K1/M (last accessed Jan. 31, 2021)

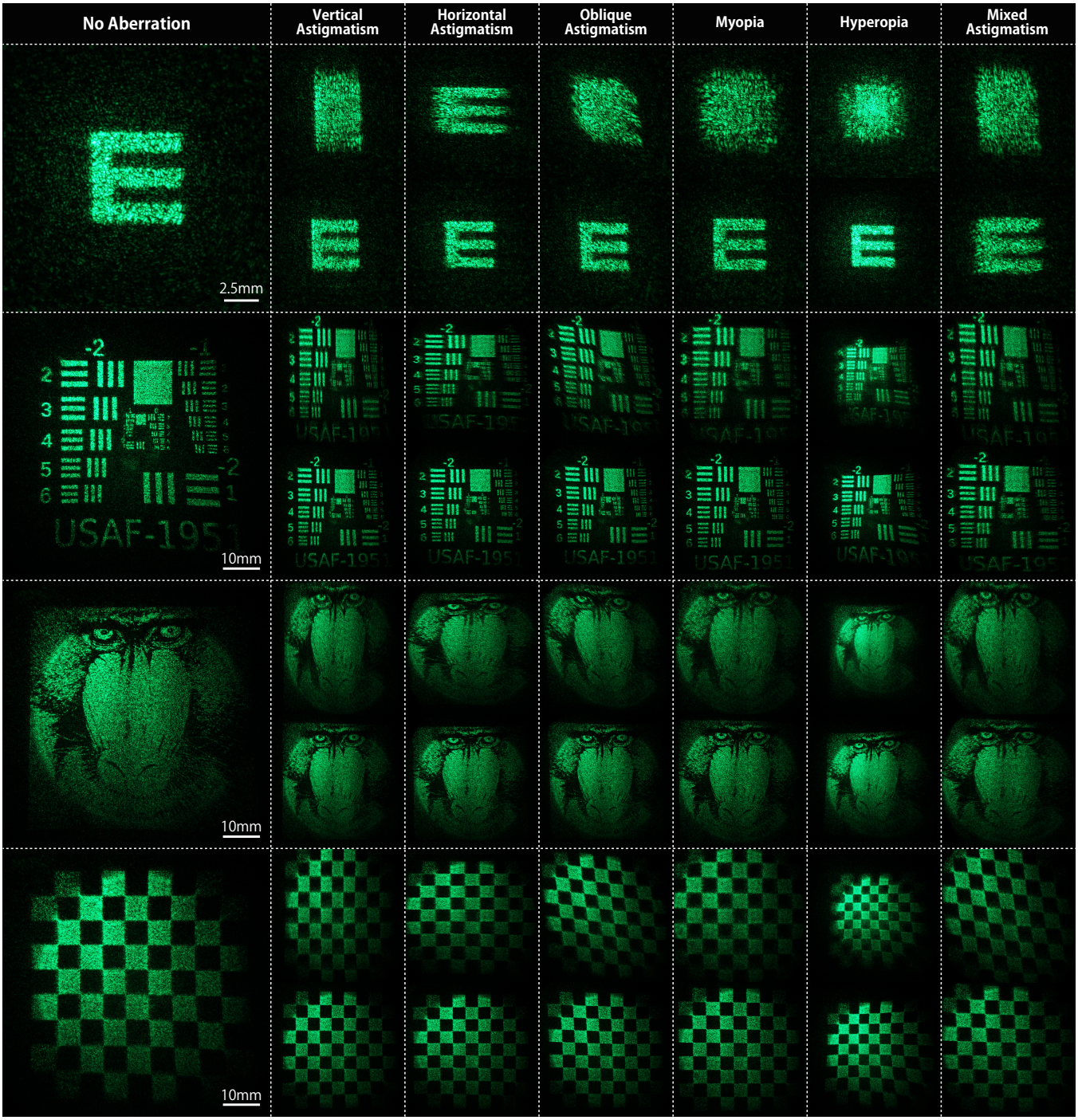

Figure 5: Display results by our HNED with and without aberration correction. The results of the aberration correction were observed in four types of images: uppercase E, USAF 1951, baboon, and checkerboard. Of the results of each aberration correction, the upper and lower column are the images before and after correction, respectively. Throughout all shooting, the camera was focused at a distance of 0.5 m with a shutter speed of 1/320 seconds. A ruler is attached to the image with no aberration as a reference size at 0.5 m. There are six types of aberrations: horizontal astigmatism, vertical astigmatism, oblique astigmatism, myopia, hyperopia, and mixed astigmatism. In all aberration patterns, the displayed image can be compensated.

displayed on the SLM included the lens pattern, the light modulated by the SLM was focused. Because the zeroth-order diffraction light was not included in the focused light, the aperture stop was set to cut off the zeroth-order light. Additionally, the first-order diffraction light from the SLM was used in this experiment because the amount of light coaxial to the optical axis was insufficient. The real image formed by the SLM lens pattern was observed using an eyepiece. The observed image was best seen when the position of the eyes was set at the focal length of the eyepiece. When reproducing aberration, an optical element (e.g., a cylindrical lens for astigmatism reproduction) was set at the position in front of the eye position.

5.2 Display Result

The change in the observed image with and without correction is depicted in Fig. 5. Images were taken with a camera (SONY ILCE-7RM2, 90 mm lens) in the position of the eyes. The aperture was open for all shots (f/2.8). This experiment considered four types of astigmatism (horizontal, vertical, oblique, and mixed), myopia, and hyperopia. When reproducing horizontal, vertical, and oblique astigmatisms, one cylindrical lens (focal length of 100 mm) was set at an angle of 0°, 90°, and 45°, respectively. To reproduce myopia and hyperopia, plano-convex and plano-concave lenses with focal lengths of 100 mm and -100 mm, respectively, were used. Mixed astigmatism was reproduced by using two cylindrical lenses with two different focal lengths (100 mm and 150 mm) set at different angles. For the sake of simplicity, only three Zernike coefficients were used in this experiment: vertical or horizontal astigmatism, myopia or hyperopia, and oblique astigmatism.

We prepared four different images with uppercase E, USAF 1951, baboon, and checkerboard, and have presented the results for each of the different aberration settings in each image. In all cases, the image form was restored to an aberration-free state, indicating that the aberrations have been corrected.

6 USER INTERFACE AND USER STUDY

In the preceding sections, we described the optics of the near-eye display, aberration correction method, and display results. In this section, we describe an interface developed to enable users to adjust the correction coefficients on their own. Additionally, we performed the experiment on humans to analyze the results of the aberration correction using the proposed interface.

6.1 User Interface

In Section 5, the correction coefficients for each aberration were adjusted to demonstrate the correction results. Our objective was to provide a simple user interface to enable the user to adjust the coefficients on their own.

Figure 6(a) depicts the image of our experimental system and the user interface. The user interface is provided and the phase calculation is processed on the same computer. The SLM is connected to the computer via an HDMI cable. The user interface has a slide bar for adjusting each coefficient, as depicted in Fig. 6(b). In this experiment, for the sake of brevity, only correction coefficients corresponding to vertical and horizontal astigmatisms, oblique astigmatism, and myopia and hyperopia were used (although it is possible to provide

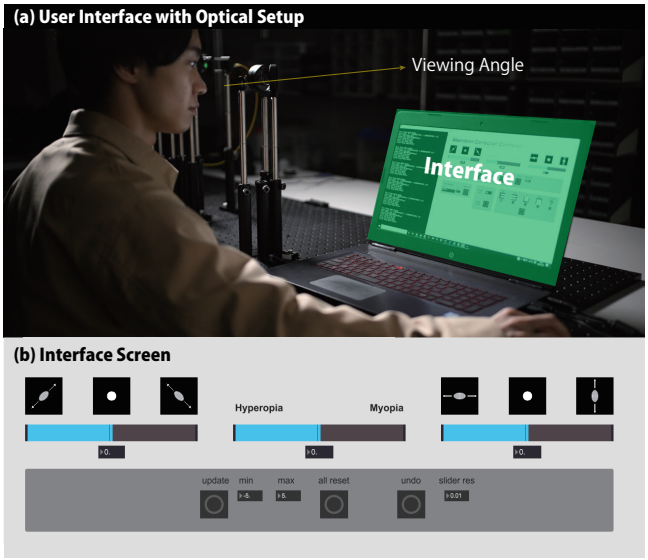

Figure 6: (a) Exterior view of the user's actual use of the interface with our HNED. (b) Screenshot of user interface used in this experiment. There are three slide bars and buttons for updating and resetting.

coefficients for higher-order aberration corrections). The user can adjust the correction coefficients by moving the slide bar, and each time the coefficients are updated by pushing the button, a process is performed to calculate the phase distribution to be displayed on the SLM. The user can repeat the adjustment of the coefficients until the image is displayed correctly.

6.2 User Study

We performed an experiment on human subjects to validate the effectiveness of the proposed method. In this section, we summarize and discuss the design and results of the experiment.

6.2.1 Tasks. We set up a visual acuity test-like task to quantify the improvement in vision after correction. The letter E, also depicted in Fig. 5, is often used in visual acuity tests [31]. In a typical visual acuity test, participants are asked to name the direction letter E is pointing toward and their visual acuity is determined from their correct responses. In this experiment, we checked the extent to which the correction improved the participants' correct response rate. The following four experimental conditions were set up.

(1) Without aberration reproduction lens (participant's naked eyes only) and without correction by HNED.
(2) Without aberration reproduction lens (participant's naked eyes only) and with correction by HNED.
(3) With aberration reproduction lens and without correction by HNED.
(4) With aberration reproduction lens and with correction by HNED.

Participants were asked to indicate the orientation (up, down, left, right) of letter E when they could recognize the letter. For the aberration reproduction lens, a cylindrical lens was used at a 45°

angle to reproduce oblique astigmatism (same settings as shown in Fig. 5). We noted the gap size of the E letter when the direction of E as answered by the participant was correct. The magnitude of E's gap size was measured by the angle of view. It was assumed that 1 arcmin (1/60°) at a distance of 5 m is equivalent to 1.454 mm, and the visual acuity of 20/20 corresponds to the visual acuity that can discriminate 1 arcmin. In this experiment, the minimum gap size to be displayed was 3.5 arcmin depending on the resolution of the display itself.

6.2.2 Procedure. Participants worked on the experiment in a room where the benchtop prototype of HNED was prepared. In the room where the experiment was conducted, the amount of light was slightly reduced such that the image displayed by the HNED could be easily seen. The participants first observed the sample image displayed by the HNED, confirmed which eye was easier to see, and decided which eye to use in the experiment. Next, they answered a pre-questionnaire about the eye they decided to use. After answering the questionnaire, they received an explanation of the experiment contents and how to use the user interface, and tried it to become familiar with the operation of the interface. The experiment was started when the participants were fully accustomed to the interface. The participants performed tasks 1 to 4 in sequence, and participants' answers and correction results were recorded. Since there were no restrictions on the number or time of trials for correction, the time used for the experiment was different for each participant; however, each experiment time for all participants was within 30 minutes.

6.2.3 Participants. In this experiment, 18 members from our laboratory were selected as participants. The participants were classified into two groups based on a pre-questionnaire. Group 1 (G1) comprised people who could manage their daily routines with their naked eyes, regardless of whether they owned glasses or contact lenses. There were nine participants (ages 20 to 26, mean 22.6±2.19) in this group, and their self-reported visual acuity had a mean of 20/19 and a standard deviation of 20/32. Group 2 (G2) comprised people who usually wore glasses and would be unable to manage their daily lives without them. There were nine participants (ages 20 to 24, mean 21.7±1.41) in this group, and their self-reported visual acuity had a mean of 20/130 and a standard deviation of 20/200. Of all participants, 12 were nearsighted, 1 participant was farsighted, and 6 participants were astigmatic. These two groups were tested under the four conditions described above.

6.2.4 Result. We verified the improvement with and without correction in the four eye conditions: good eyesight, good eyesight + oblique astigmatism, poor eyesight, and poor eyesight + oblique astigmatism. The boxplots for each group are depicted in Fig. 7 for the minimum gap size of the discriminable letter E measured under each experimental condition. The Wilcoxon rank sum test was used to analyze the experimental results before and after the correction with a significant difference of 5%. In G1, there was no significant difference between tasks 1 and 2 in the Wilcoxon test ($p = 0.1573$), because users with good eyesight could see the smallest size on the display, and there was no improvement from the correction. In contrast, we see an improvement between tasks 3 and 4 with the aberration reproduction lenses, with a significant difference

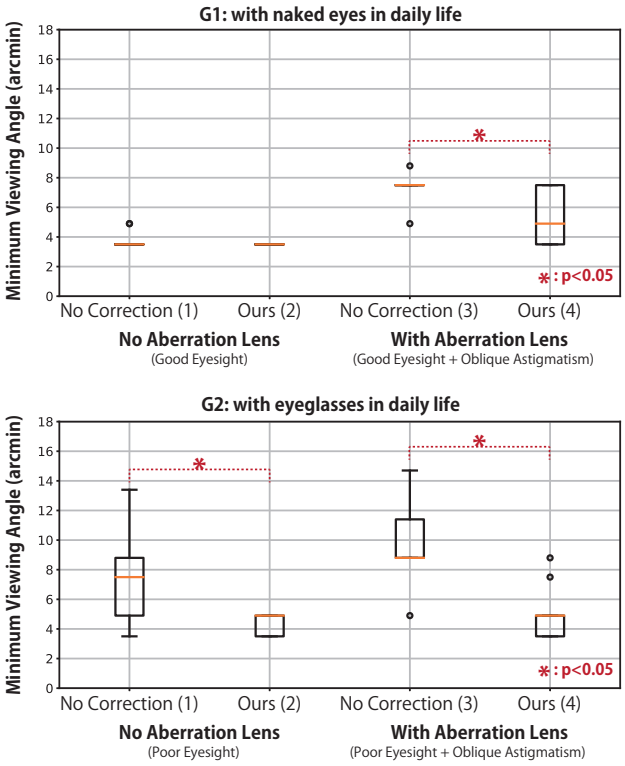

Figure 7: Boxplots of the results of the experiment. The orange line represents the median, box represents the quartile range, whiskers indicate minimum and maximum, and dots indicate the outliers.

in the Wilcoxon test ($p = 0.0412$). In G2, there was a significant difference between tasks 1 and 2 ($p = 0.0277$) and between tasks 3 and 4 ($p = 0.0112$).

These results indicate that the proposed correction interface is effective. In particular, the significant difference between tasks 1 and 2 in G2 is an important result that demonstrates the usefulness of the proposed method in correcting the visibility even for the naked eyes of users with poor eyesight.

7 DISCUSSION

7.1 Aberration-Correctable Holographic Near-Eye Display

7.1.1 Image Distortion Independent of Focal Length. Many near-eye displays use eyepieces, and the optics that place the eye at the focus of the eyepiece are known as the Maxwellian view display or retinal display [20, 24, 42, 43]. The Maxwellian-type near-eye display has the advantage of displaying images independent of the focal length of the eye. By aligning the light path to the center of the pupil, the display is not affected by the eye. However, these displays are not completely free from eye aberrations. For example, Takaki et al. [43] demonstrated the need to consider the effect of astigmatism. In our experiments, we also found that people with severely impaired eyesight are affected by eye aberrations.

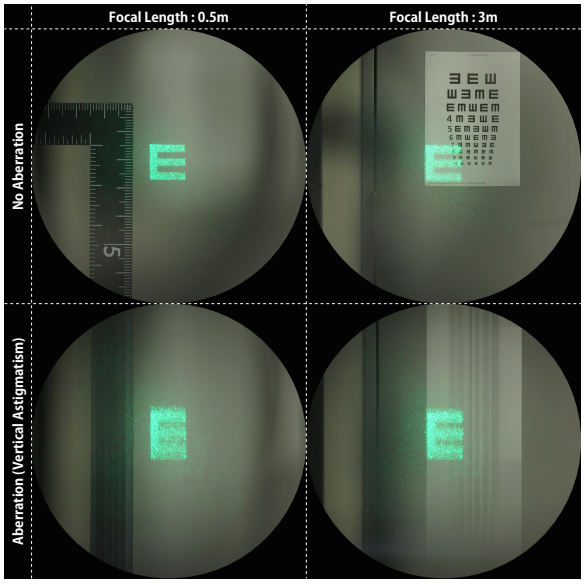

Figure 8: Images depicting the characteristics of the Maxwellian view. The upper and lower columns depict the images without and with an aberration-reproducing lens, respectively.

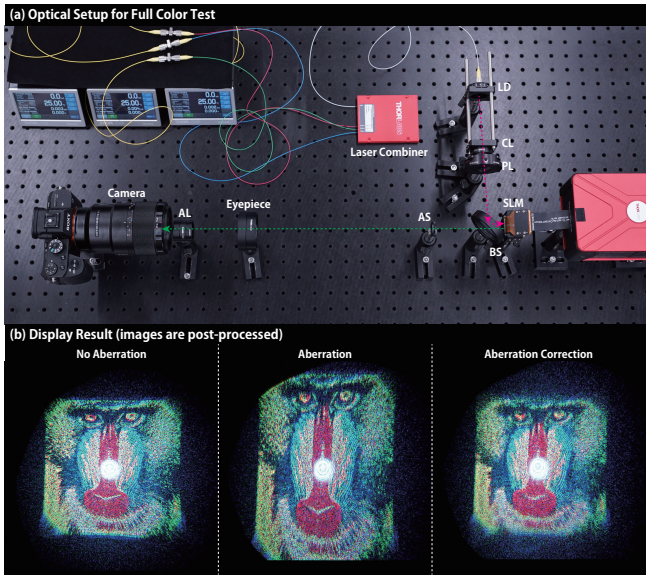

Figure 9: (a) An image of the optical system used in the full-color experiment. (b) Results of aberration correction in the full-color experiment. All images were post-processed from the images taken at each RGB wavelength.

To investigate the relationship between the aberration and Maxwellian view in the optical system, we observed the images at different focal positions through an aberration reproduction lens (a cylindrical lens with a focal length of 100 mm for vertical astigmatism reproduction). Figure 8 depicts the results with and without an aberration reproduction lens. Under both conditions, the image does not depend on the focal length; in the presence of the aberration, the image is blurred even when the focal length is changed.

However, it is also true that the images produced by the Maxwellian view are not affected easily by aberrations. Therefore, although the proposed optical system is considered to be a Maxwellian-type near-eye display, the discussion of aberrations is essential.

7.1.2 Full-Color HNED. In this study, we focused on monochromatic aberrations only because we used only one laser wavelength for HNED. Colorization is an essential element in enriching HNED. Therefore, we performed an experiment on aberration correction in full-color HNED, taking pictures for each RGB wavelength and postprocessing them to simulate a full-color display. The exposure time of each image was 1/320 seconds, and images were displayed at 30 Hz on the SLM. The optical system used in the full-color experiment is depicted in Fig. 9(a). A laser combiner was used to unify the optical axes at all wavelengths, and a cylindrical lens with a focal length of 100 mm was used to reproduce the aberration.

Figure 9(b) depicts the results before and after the aberration correction. The same correction factors were used for aberration correction for all wavelengths. It is evident that aberration correction works even when the same correction factors are used. In the future, more detailed aberration correction will be required for each wavelength, and a higher frame rate of SLM will enable full-color observation.

7.1.3 Computer-Generated Hologram. The DPAC method was employed in this study to achieve a fast phase calculation. However, in principle, this method causes a reduction in the intensity of light [39]. In the DPAC method, a checkerboard pattern of phases on the SLM causes diffraction images and light dispersion. In the experiment by Peng et al. [39], the diffraction image was ignored and only the image generated coaxially with the optical axis was utilized. However, in our setup, the amount of light in the image on the optical axis is extremely low owing to the use of the SLM with a smaller pitch size; hence, we only used the diffracted image.

To avoid these problems, a high-precision phase calculation method without a periodic structure is required. If interactive computation is required, it is necessary to perform the most appropriate phase computation based on the coefficient input by the user. Therefore, it is possible to build a neural network architecture with user-defined aberration correction coefficients in the future.

7.1.4 Optical Hardware Considerations. In this study, we added a lens pattern to the phase pattern displayed on the SLM for cutting the zeroth-order light. In this design, the distance from the SLM to the image plane is required, which increases the optical path length and enlarges the optical system. To realize spectacle-type devices for augmented reality in the future, it is necessary to optimize the phase distribution and miniaturize the optical design. For example, if the phase distribution displayed on the SLM is close to the real image for the observation and the holographic optical element (HOE) is placed at the position of the lens of the glasses as an eyepiece, miniaturization can be achieved.

In addition, when the proposed HNED is used as a see-through type, the visual field image of the outside world must also be corrected. The optical design of near-eye displays to address this issue has begun to be discussed in some studies [48, 51]. In HNED as well, it will be necessary in the future to deal with the problem by properly designing the spectacle layer and the HOE layer.

7.2 User Interface

The results in Section 6.2.4 demonstrate that aberration correction via our interface was useful. However, further improvements to the proposed method are necessary. We discuss these improvements in this section.

7.2.1 Exploring Optimal Coefficients Values. The most important drawback is that the user may not be able to reach the appropriate coefficients in some cases. Although our interface allows users to adjust the coefficients by moving the slide bar freely, the search for the appropriate coefficients requires many trials. In our experiment, some users gave up adjusting the correction because the search was unsuccessful. The key to solving this problem is to make the search easy and accurate for users. For example, opticians use the staircase method to determine the optimal spectacle lens based on user feedback. There are also studies of treating users as a black box or as a function that can answer only likes and dislikes, and reducing the number of user feedback by inferring appropriate coefficients from the few responses [8, 25]. In the HNED, there can also be a method to search for coefficients by showing users some correction results and having them provide feedback on the quality of the adjustment results.

7.2.2 Calculation Time and Interactivity. As mentioned before, some people quit the search for the correction coefficient. This withdrawal may be due to the time required for a single attempt. In this experiment, the phase calculation to update the coefficients took approximately 4 seconds, and we had to specify the coefficients and then press the update button to reflect the correction result. We need to reduce the calculation time to be able to see the result of the correction synchronized with the slide bar movement.

8 CONCLUSION

In this study, we proposed an HNED with an interactive aberration correction mechanism. We developed a correction method for individual eye aberrations, which has not been studied thoroughly in the past. To develop an HNED that can compensate for eye aberrations, we formulated light propagation including eyes with aberrations to enable phase calculation for HNED. Additionally, we developed a GUI that can work with the HNED to enable the user to make his or her own corrections because eye aberrations differ from individual to individual. This interface enables the user to search for the best aberration correction on their own. We performed an experiment in which individuals with good and poor eyesight were invited to participate to validate the proposed method. We found that the aberration correction using our interface can help make images discriminable.

In the future, it will be necessary to propose a method to perform more detailed aberration correction while reducing the time burden on the user. Furthermore, a method of aberration correction for other types of HNED will also be required. We believe that our formulation of the problem and our correction method will be useful for designing these aberration correction methods in the future.

ACKNOWLEDGMENTS

This research was supported by Pixie Dust Technologies, Inc., and we would like to thank So Nishimura for his many advices.

REFERENCES

[1] David J. Apple, Nick Mamalis, Katherine Loftfield, Joseph M. Googe, Linda C. Novak, Dolores Kavka-Van Norman, Steven E. Brady, and Randall J. Olson. 1984. Complications of intraocular lenses. A historical and histopathological review. *Survey of Ophthalmology* 29, 1 (1984), 1 – 54. https://doi.org/10.1016/0039-6257(84)90113-9

[2] David J. Apple, Kerry D. Solomon, Manfred R. Tetz, Ehud I. Assia, Elizabeth Y. Holland, Ulrich F.C. Legler, Julie C. Tsai, Victoria E. Castaneda, Judy P. Hoggatt, and Alexandra M.P. Kostick. 1992. Posterior capsule opacification. *Survey of Ophthalmology* 37, 2 (1992), 73 – 116. https://doi.org/10.1016/0039-6257(92)90073-3

[3] Brian A. Barsky. 2004. Vision-Realistic Rendering: Simulation of the Scanned Foveal Image from Wavefront Data of Human Subjects. In *Proceedings of the 1st Symposium on Applied Perception in Graphics and Visualization (APGV '04)*. Association for Computing Machinery, New York, NY, USA, 73–81. https://doi.org/10.1145/1012551.1012564

[4] Carmen Cánovas, Pedro M. Prieto, Silvestre Manzanera, Alejandro Mira, and Pablo Artal. 2010. Hybrid adaptive-optics visual simulator. *Opt. Lett.* 35, 2 (Jan 2010), 196–198. https://doi.org/10.1364/OL.35.000196

[5] Praneeth Chakravarthula, Ethan Tseng, Tarun Srivastava, Henry Fuchs, and Felix Heide. 2020. Learned Hardware-in-the-loop Phase Retrieval for Holographic Near-Eye Displays. *ACM Transactions on Graphics (TOG)* 39, 6 (2020), 186.

[6] Steven A. Cholewiak, Gordon D. Love, and Martin S. Banks. 2018. Creating correct blur and its effect on accommodation. *Journal of Vision* 18, 9 (09 2018), 1–1. https://doi.org/10.1167/18.9.1 arXiv:https://arvojournals.org/arvo/content_public/journal/jov/937491/i1534-7362-18-9-1.pdf

[7] Steven A. Cholewiak, Gordon D. Love, Pratul P. Srinivasan, Ren Ng, and Martin S. Banks. 2017. Chromablur: Rendering Chromatic Eye Aberration Improves Accommodation and Realism. *ACM Trans. Graph.* 36, 6, Article 210 (Nov. 2017), 12 pages. https://doi.org/10.1145/3130800.3130815

[8] Brochu Eric, Nando Freitas, and Abhijeet Ghosh. 2008. Active Preference Learning with Discrete Choice Data. In *Advances in Neural Information Processing Systems*, J. Platt, D. Koller, Y. Singer, and S. Roweis (Eds.), Vol. 20. Curran Associates, Inc., 409–416. https://proceedings.neurips.cc/paper/2007/file/b6a1085a27ab7bff7550f8a3bd017df8-Paper.pdf

[9] Enrique Josua Fernández. 2012. Adaptive optics for visual simulation. *International Scholarly Research Notices* 2012 (2012).

[10] Enrique J. Fernández, Ignacio Iglesias, and Pablo Artal. 2001. Closed-loop adaptive optics in the human eye. *Opt. Lett.* 26, 10 (May 2001), 746–748. https://doi.org/10.1364/OL.26.000746

[11] Qiankun Gao, Juan Liu, Xinhui Duan, Tao Zhao, Xin Li, and Peilin Liu. 2017. Compact see-through 3D head-mounted display based on wavefront modulation with holographic grating filter. *Opt. Express* 25, 7 (Apr 2017), 8412–8424. https://doi.org/10.1364/OE.25.008412

[12] Heidi Hofer, Pablo Artal, Ben Singer, Juan Luis Aragón, and David R. Williams. 2001. Dynamics of the eye's wave aberration. *J. Opt. Soc. Am. A* 18, 3 (Mar 2001), 497–506. https://doi.org/10.1364/JOSAA.18.000497

[13] B Howland and HC Howland. 1976. Subjective measurement of high-order aberrations of the eye. *Science* 193, 4253 (1976), 580–582. https://doi.org/10.1126/science.959814 arXiv:https://science.sciencemag.org/content/193/4253/580.full.pdf

[14] Howard C. Howland and Bradford Howland. 1977. A subjective method for the measurement of monochromatic∗ aberrations of the eye. *J. Opt. Soc. Am.* 67, 11 (Nov 1977), 1508–1518. https://doi.org/10.1364/JOSA.67.001508

[15] C. K. Hsueh and A. A. Sawchuk. 1978. Computer-generated double-phase holograms. *Appl. Opt.* 17, 24 (Dec 1978), 3874–3883. https://doi.org/10.1364/AO.17.003874

[16] Fu-Chung Huang and Brian A. Barsky. 2011. *A Framework for Aberration Compensated Displays.* Technical Report UCB/EECS-2011-162. EECS Department, University of California, Berkeley. http://www2.eecs.berkeley.edu/Pubs/TechRpts/2011/EECS-2011-162.html

[17] Fu-Chung Huang, Douglas Lanman, Brian A. Barsky, and Ramesh Raskar. 2012. Correcting for Optical Aberrations Using Multilayer Displays. *ACM Trans. Graph.* 31, 6, Article 185 (Nov. 2012), 12 pages. https://doi.org/10.1145/2366145.2366204

[18] Fu-Chung Huang, Gordon Wetzstein, Brian A. Barsky, and Ramesh Raskar. 2014. Eyeglasses-Free Display: Towards Correcting Visual Aberrations with Computational Light Field Displays. *ACM Trans. Graph.* 33, 4, Article 59 (July 2014), 12 pages. https://doi.org/10.1145/2601097.2601122

[19] Yuta Itoh and Gudrun Klinker. 2015. Vision Enhancement: Defocus Correction via Optical See-through Head-Mounted Displays. In *Proceedings of the 6th Augmented Human International Conference (AH '15)*. Association for Computing Machinery, New York, NY, USA, 1–8. https://doi.org/10.1145/2735711.2735787

[20] Changwon Jang, Kiseung Bang, Seokil Moon, Jonghyun Kim, Seungjae Lee, and Byoungho Lee. 2017. Retinal 3D: Augmented Reality near-Eye Display via Pupil-Tracked Light Field Projection on Retina. *ACM Trans. Graph.* 36, 6, Article 190 (Nov. 2017), 13 pages. https://doi.org/10.1145/3130800.3130889

[21] Masanori Kakimoto, Tomoaki Tatsukawa, Yukiteru Mukai, and Tomoyuki Nishita. 2007. Interactive Simulation of the Human Eye Depth of Field and Its Correction by Spectacle Lenses. *Computer Graphics Forum* 26, 3 (2007), 627–636. https://doi.org/10.1111/j.1467-8659.2007.01086.x arXiv:https://onlinelibrary.wiley.com/doi/pdf/10.1111/j.1467-8659.2007.01086.x

[22] Dongyeon Kim, Kiseung Bang, Youngmo Jeong, and Byoungho Lee. 2019. Compensating high-order optical aberrations induced by abnormal shape of cornea in holographic displays, In Frontiers in Optics + Laser Science APS/DLS. *Frontiers in Optics + Laser Science APS/DLS*, JW4A.102. https://doi.org/10.1364/FIO.2019.JW4A.102

[23] Dongyeon Kim, Seung-Woo Nam, Kiseung Bang, and Byoungho Lee. 2020. P-81: Holographic Near-to-Eye Display for Vision-Correcting Application. *SID Symposium Digest of Technical Papers* 51, 1 (2020), 1660–1663. https://doi.org/10.1002/sdtp.14214 arXiv:https://onlinelibrary.wiley.com/doi/pdf/10.1002/sdtp.14214

[24] Seong-Bok Kim and Jae-Hyeung Park. 2018. Optical see-through Maxwellian near-to-eye display with an enlarged eyebox. *Opt. Lett.* 43, 4 (Feb 2018), 767–770. https://doi.org/10.1364/OL.43.000767

[25] Yuki Koyama, Issei Sato, and Masataka Goto. 2020. Sequential Gallery for Interactive Visual Design Optimization. *ACM Trans. Graph.* 39, 4, Article 88 (July 2020), 12 pages. https://doi.org/10.1145/3386569.3392444

[26] Jin Su Lee, Yoo Kwang Kim, and Yong Hyub Won. 2018. See-through display combined with holographic display and Maxwellian display using switchable holographic optical element based on liquid lens. *Opt. Express* 26, 15 (Jul 2018), 19341–19355. https://doi.org/10.1364/OE.26.019341

[27] Junzhong Liang, Bernhard Grimm, Stefan Goelz, and Josef F. Bille. 1994. Objective measurement of wave aberrations of the human eye with the use of a Hartmann–Shack wave-front sensor. *J. Opt. Soc. Am. A* 11, 7 (Jul 1994), 1949–1957. https://doi.org/10.1364/JOSAA.11.001949

[28] Junzhong Liang and David R. Williams. 1997. Aberrations and retinal image quality of the normal human eye. *J. Opt. Soc. Am. A* 14, 11 (Nov 1997), 2873–2883. https://doi.org/10.1364/JOSAA.14.002873

[29] Wen-Kai Lin, Osamu Matoba, Bor-Shyh Lin, and Wei-Chia Su. 2018. Astigmatism and deformation correction for a holographic head-mounted display with a wedge-shaped holographic waveguide. *Appl. Opt.* 57, 25 (Sep 2018), 7094–7101. https://doi.org/10.1364/AO.57.007094

[30] Jung-Ping Liu, Wang-Yu Hsieh, Ting-Chung Poon, and Peter Tsang. 2011. Complex Fresnel hologram display using a single SLM. *Appl. Opt.* 50, 34 (Dec 2011), H128–H135. https://doi.org/10.1364/AO.50.00H128

[31] Jan E Lovie-Kitchin. 1988. Validity and reliability of visual acuity measurements. *Ophthalmic and physiological optics* 8, 4 (1988), 363–370.

[32] Andrew Maimone, Andreas Georgiou, and Joel S. Kollin. 2017. Holographic Near-Eye Displays for Virtual and Augmented Reality. *ACM Trans. Graph.* 36, 4, Article 85 (July 2017), 16 pages. https://doi.org/10.1145/3072959.3073624

[33] Samir A Melki and Dimitri T Azar. 2001. LASIK Complications: Etiology, Management, and Prevention. *Survey of Ophthalmology* 46, 2 (2001), 95 – 116. https://doi.org/10.1016/S0039-6257(01)00254-5

[34] Seung-Woo Nam, Seokil Moon, Byounghyo Lee, Dongyeon Kim, Seungjae Lee, Chang-Kun Lee, and Byoungho Lee. 2020. Aberration-corrected full-color holographic augmented reality near-eye display using a Pancharatnam-Berry phase lens. *Opt. Express* 28, 21 (Oct 2020), 30836–30850. https://doi.org/10.1364/OE.405131

[35] Rafael Navarro, Esther Moreno-Barriuso, Salvador Bará, and Teresa Mancebo. 2000. Phase plates for wave-aberration compensation in the human eye. *Opt. Lett.* 25, 4 (Feb 2000), 236–238. https://doi.org/10.1364/OL.25.000236

[36] Paul C. Nicolson and Jürgen Vogt. 2001. Soft contact lens polymers: an evolution. *Biomaterials* 22, 24 (2001), 3273 – 3283. https://doi.org/10.1016/S0142-9612(01)00165-X Opthalmic Special Issue.

[37] Matthias Nießner, Roman Sturm, and Günther Greiner. 2012. Real-time simulation and visualization of human vision through eyeglasses on the GPU. In *Proceedings of the 11th ACM SIGGRAPH International Conference on Virtual-Reality Continuum and its Applications in Industry*. 195–202.

[38] Vitor F. Pamplona, Manuel M. Oliveira, Daniel G. Aliaga, and Ramesh Raskar. 2012. Tailored Displays to Compensate for Visual Aberrations. *ACM Trans. Graph.* 31, 4, Article 81 (July 2012), 12 pages. https://doi.org/10.1145/2185520.2185577

[39] Yifan Peng, Suyeon Choi, Nitish Padmanaban, and Gordon Wetzstein. 2020. Neural Holography with Camera-in-the-loop Training. *ACM Trans. Graph. (SIGGRAPH Asia)* (2020).

[40] Jason Porter, Antonio Guirao, Ian G. Cox, and David R. Williams. 2001. Monochromatic aberrations of the human eye in a large population. *J. Opt. Soc. Am. A* 18, 8 (Aug 2001), 1793–1803. https://doi.org/10.1364/JOSAA.18.001793

[41] Nikolai Suchkov, Enrique J. Fernández, and Pablo Artal. 2019. Wide-range adaptive optics visual simulator with a tunable lens. *J. Opt. Soc. Am. A* 36, 5 (May 2019), 722–730. https://doi.org/10.1364/JOSAA.36.000722

[42] Mitsuru Sugawara, Makoto Suzuki, and Nori Miyauchi. 2016. 14-5L: Late-News Paper: Retinal Imaging Laser Eyewear with Focus-Free and Augmented Reality. *SID Symposium Digest of Technical Papers* 47, 1 (2016), 164–167. https://doi.org/10.1002/sdtp.10626 arXiv:https://onlinelibrary.wiley.com/doi/pdf/10.1002/sdtp.10626

[43] Yasuhiro Takaki and Naohiro Fujimoto. 2018. Flexible retinal image formation by holographic Maxwellian-view display. *Opt. Express* 26, 18 (Sep 2018), 22985–22999. https://doi.org/10.1364/OE.26.022985

[44] Kevin M Tuohy. 1950. Contact lens. US Patent 2,510,438.

[45] Gert Van den Brink. 1962. Measurements of the geometrical aberrations of the eye. *Vision Research* 2, 7-8 (1962), 233–244.

[46] Douglas G Vanderlaan, Ivan M Nunez, Marcie Hargiss, Michele L Alton, and Susan Williams. 1999. Soft contact lenses. US Patent 5,998,498.

[47] Andrew B. Watson. 2015. Computing human optical point spread functions. *Journal of Vision* 15, 2 (02 2015), 26–26. https://doi.org/10.1167/15.2.26 arXiv:https://arvojournals.org/arvo/content_public/journal/jov/933690/i1534-7362-15-2-26.pdf

[48] Yishi Wu, Chao Ping Chen, Lei Zhou, Yang Li, Bing Yu, and Huayi Jin. 2017. Design of see-through near-eye display for presbyopia. *Opt. Express* 25, 8 (Apr 2017), 8937–8949. https://doi.org/10.1364/OE.25.008937

[49] Han-Ju Yeom, Hee-Jae Kim, Seong-Bok Kim, HuiJun Zhang, BoNi Li, Yeong-Min Ji, Sang-Hoo Kim, and Jae-Hyeung Park. 2015. 3D holographic head mounted display using holographic optical elements with astigmatism aberration compensation. *Opt. Express* 23, 25 (Dec 2015), 32025–32034. https://doi.org/10.1364/OE.23.032025

[50] Thomas Young. 1801. II. The Bakerian Lecture. On the mechanism of the eye. *Philosophical Transactions of the Royal Society of London* 91 (1801), 23–88.

[51] Lei Zhou, Chao Ping Chen, Yishi Wu, Zhonglin Zhang, Keyu Wang, Bing Yu, and Yang Li. 2017. See-through near-eye displays enabling vision correction. *Opt. Express* 25, 3 (Feb 2017), 2130–2142. https://doi.org/10.1364/OE.25.002130